

Ligature Instabilities in the Perceptual Organization of Shape

Jonas August

Department of Electrical Engineering, Yale University, New Haven, Connecticut 06520

Kaleem Siddiqi

School of Computer Science, McGill University, Montréal, Québec, Canada H3A 2A7

and

Steven W. Zucker¹

Departments of Computer Science and Electrical Engineering, Yale University, New Haven, Connecticut 06520

Received September 13, 1999; accepted September 13, 1999

Although the classical Blum skeleton has long been considered unstable, many have attempted to alleviate this defect through pruning. Unfortunately, these methods have an arbitrary basis, and, more importantly, they do not prevent internal structural alterations due to slight changes in an object's boundary. The result is a relative lack of development of skeleton representations for indexing object databases, despite a long history. Here we revisit a subset of the skeleton—called ligature by Blum—to demonstrate how the topological sensitivity of the skeleton can be alleviated. In particular, we show how the deletion of ligature regions leads to stable hierarchical descriptions, illustrating this point with several computational examples. We then relate ligature to a natural growth principle to provide an account of the perceptual parts of shape. Finally, we discuss the duality between the problems of part decomposition and contour fragment grouping. © 1999 Academic Press

1. INTRODUCTION

The analysis of visual shape is one of the most controversial areas of computer vision, and perhaps nowhere is this better articulated than in the questions surrounding the organization of object databases. The basic question—"Which properties of shape should provide the basis for representation?"—is alternatively governed by (i) the *reliability* of computing the representation and (ii) how it should be *organized* to facilitate search. While these motivations are clearly interrelated, they are often interpreted by researchers to point in opposite directions. The reliability question is taken to imply that, since "edge" maps are never perfect, one should focus on appearance; on the other hand, the organizational question seeks abstractions that can be

organized into hierarchies to support search. Appearance representations [22], it is therefore widely held, should be intensity-based, while abstractions such as skeletons [6, 24], shocks [17], and part primitives [4], from which organizational hierarchies can be built, are in practice not computable.

A consequence of this tension is the shape dilemma: computable iconic representations do not support shape-based indexing abstractions; and structural abstractions are not computable from images. To elaborate, appearance-based representations are naturally suited to finding an instance in a database of instances, such as da Vinci's face in a database of normalized, cropped faces; but these are all in the same generic class. In contrast, structural hierarchies provide a kind of "Dewey decimal system" for objects (the torso supports a head and arms; each arm consists of an upper and lower portion; the lower portion consists of forearm, wrist, and hand; the hand consists of palm and fingers, and so on) [21, p. 306].

The difficulties in computing abstractions for skeletons are illustrative of the second side of the above dilemma, and in our view have played a central role in casting doubt on them. We shall argue in this paper that they can be overcome in a manner that is both natural and computable.

In Fig. 1 we show a rectangle, and another rectangle, with a small "glitch." Clearly, the glitch has a disproportionate effect on the skeleton [25, p. 506], producing a new branch of substantial length. The entire notion of hierarchy for such descriptions is therefore cast in doubt because shapes exist for which small changes in the outline imply large changes in the skeleton. These kinds of examples prompted Marr to formulate a stability requirement for shape representations: small changes in a shape should result in small changes in its representation [21].

We submit that there is a natural principle by which the glitch-branch can be separated from the rest of the skeleton in this example, and that this principle is fundamentally related to abstractions of shape. The basic idea is illustrated in Fig. 2, where we

¹ To whom all correspondence should be addressed at Yale University, P.O. Box 208285, Yale Station, New Haven, CT 06520-8285. Fax: (203)432-0593. E-mail: steven.zucker@yale.edu.



FIG. 1. (Left) Rectangle with skeleton. The addition of a “glitch” (center) adds a whole new skeleton branch, but ligature (white, see Section 2) links a *local* glitch description to that of the rectangle (right).

introduce the notion of the ligature² as the “glue” that holds the limb onto the rectangle. While the formal definitions appear later in the paper, notice how the labeling of the ligature regions identifies how the “glitch” is attached to the rectangle (Fig. 1, right).

Boundary glitches are only one example of what can be cited as instabilities in skeletons, because they correspond to those branches that terminate. (Indeed, most attempts to prune [24, 27] the skeleton explicitly work inward from branch endpoints.) What appears at first to be another, totally unrelated instability occurs for *interior* branches of more complex skeletons (Fig. 10). As stated above, hands can be described as palms with finger protrusions. However, small changes in the hand can give rise to large changes in the skeletal branching pattern between the palm and the fingers. Somehow these changes must be signalled as insignificant with respect to the shape. Again, ligature is relevant.

In summary, our claim in this paper is that ligature signals those portions of the skeleton that can be unstable. In effect, these unstable components must be labeled as such, so that they do not dominate the shape-matching process. Boundary glitches may, however, have significance, as for example when they represent tails and limbs. Ligature is important for signaling these part-events as well.

Although we shall not develop the connection in this paper, we comment that one way to formulate shape descriptions for matching is to organize them into a significance hierarchy [30], where significance derives from a hyperbolic curve evolution process [17]. The shocks of this process trace out the locus of skeleton positions and also label them with (a) time of formation and (b) type of singularity. The resultant trees place the most significant nodes (the last to form, in evolutionary time) toward the root (e.g., the torso and head for a person), while the least significant ones are nearer to the leaves. The ligature computations in this paper can be made in parallel with the shock descriptions and will extend the significance notion beyond that of time-of-formation. At the end of this paper we make several comments about stable object descriptions and how ligature and shocks can work together. Axial descriptions for graph-based shape representation and matching have also been explored in [20, 28].

The paper is organized as follows. We next define skeleton and ligature (Section 2) and then show how to compute it (Section 3). Mating ligature to shock-based descriptions, we illustrate the natural variations that occur within a typical shape category with several examples of hands, and how ligature re-

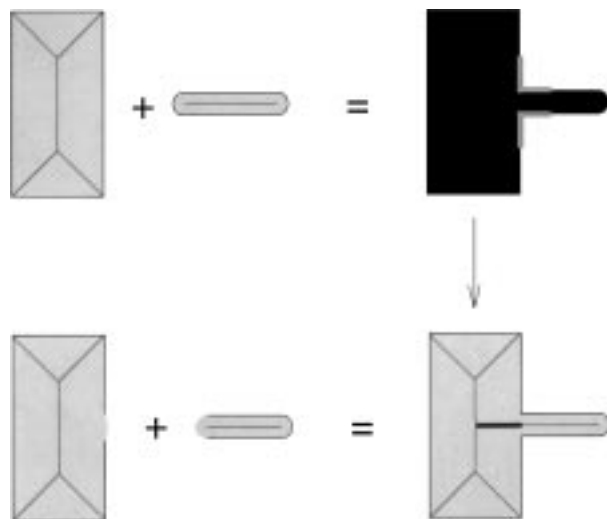


FIG. 2. Part decomposition via ligature. A horizontal sausage and a vertical rectangle with their skeletons (top left) are combined to form a single whole (top right). Observe the formation of the two concave corners (in grey). (Bottom right) The skeleton of the silhouette has a component which is related to the concave corners and is called ligature (shown in thick black). Note that the ligature *links* the skeleton on the left, which resembles the skeleton of the unpenetrated rectangle, *to* the skeleton on the right, which resembles the skeleton of the unpenetrated sausage. By removing this ligature, the remaining skeleton has two components, each of which serves to approximate one of the original objects which were combined (bottom left).

mains concentrated on the unstable “web” portion of it. Several other computations (Section 4) also demonstrate the improved stability of our representation. We then show in Section 5 how ligature provides a new geometry for part decomposition and we interpret ligature as evidence of part growth. Finally, we observe in Section 6 a duality between the problems of part decomposition and contour fragment grouping.

2. BLUM'S SKELETON AND LIGATURE

Recall the definition of the skeleton [6] of a bounded open set $A \subset \mathbb{R}^2$ in terms of *maximal open disks*, where an open disk B is maximal in A iff there exists no other open disk $B' \subset A$ such that B is strictly contained in B' :

DEFINITION 1 (Blum). The *skeleton* S of A is the set of centers of maximal open disks contained in A .

The *projection* $\pi(x)$ is the set of points in the boundary ∂A of A closest to x , or $\pi(x) \triangleq \{p \in \partial A : \|x - p\| = \rho(x)\}$, where $\rho(x) = \min\{\|x - p\| : p \in \partial A\}$ is the radius function. For skeleton point $q \in S$, $\pi(q)$ is the set³ of boundary points “touched” by the maximal disk at q , and thus the projection relates skeleton to boundary points.

As is classical in vision [14], negative minima of curvature of an object’s boundary play a role in the perceptual organization

² After discovery by Blum [6], ligature was next used in [1].

³ $|\pi(q)| = 2$, except at junctions ($|\pi(q)| = 3$, generically) or branch endpoints ($|\pi(q)| = 1$).

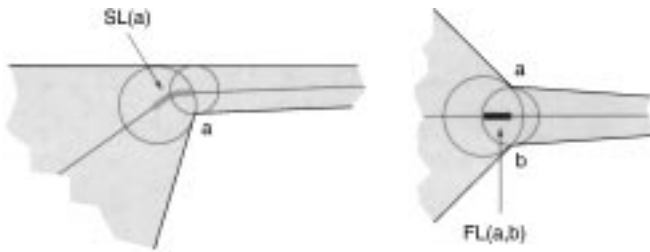


FIG. 3. (Left) The semiligature $SL(a)$ with respect to concave corner a . Observe that the maximal disks centered at the ends of $SL(a)$ touch a and the top boundary (noncorner). (Right) The full ligature $FL(a, b)$ with respect to concave corners a and b . The maximal disks centered at the ends of $FL(a, b)$ touch a and b .

of shape. For simplicity, consider the idealized situation where these minima are concave corners, and let V denote the set of all such orientation discontinuities. Now for a given object A with skeleton S , consider those skeletal points q whose maximal disks touch some concave corner; Blum [6] dubbed such q *ligature*.⁴ Those skeletal points related to only one concave corner form semiligature:

DEFINITION 2. The *semiligature* with respect to a $a \in V$:

$$SL(a) \triangleq \{q \in S : \pi(q) = \{a, p\} \text{ and } p \notin V\}.$$

See Fig. 3. Note that the semiligature with respect to a given concave corner may not be a connected set (Fig. 15). Full ligature comprises those skeletal points related to two concave corners.

DEFINITION 3. The *full ligature* with respect to $a, b \in V$:

$$FL(a, b) \triangleq \{q \in S : \pi(q) \supset \{a, b\}\}.$$

Note that $FL(a, b) = FL(b, a)$. Full ligature has the following properties:

Property 1. $FL(a, b)$ lies along a straight line.

Property 2. $FL(a, b)$ is a connected set.

Property 3. Barring degeneracies,^{4a} $FL(a, b)$ has nonzero length.

These properties clearly hold in Fig. 3, and they follow directly from a formal analogy⁵ with gap skeleton [1], which arises in contour fragment grouping.

⁴ Blum chose the word ligature well. According to Webster's dictionary, *ligature* means "Something, as a cord or wire, that ties or binds."

^{4a} See Prop. 3 in [2] for analogous degeneracy condition.

⁵ Compare the definitions of full ligature here and in [2] substitute A (object) and "endpoint," here, resp., for the complement of A (the background space among a set of contour fragments) and "concave corner," in [2], resp., except that the containment relation $\pi(q) \supset \{a, b\}$ (introduced here to ensure that junction points are not excluded from $FL(a, b)$) is replaced with equality. Thus full ligature here may in a degenerate case be only one point: consider the case where one of the two tangents in a small neighborhood of each of the corners a and b is tangent to the maximal disk at $q \in FL(a, b)$, but that these two tangents are not mirror symmetric in tangent line to the skeleton at q . Gap skeleton is described in Section 6.

3. COMPUTING STABLE DESCRIPTIONS: BENDS, SEEDS, AND LIGATURE

The skeleton described in the previous section also arises in a more general theory of curve evolution. Capturing the principle that similar (planar) shapes should be bounded by similar curves, the evolutionary approach to shape description introduces the partial differential equation [17]

$$\frac{\partial C}{\partial t} = \beta N, \quad (1)$$

with the initial condition $C(s, 0) = C_0(s)$ (the boundary of the object at the start of the evolution), where $C(\cdot, t)$ is the closed curve describing the boundary of the shape after being deformed for time t , N is the boundary normal, s is the parameter along the boundary, and β is any function $\beta(\kappa)$ of curvature κ . The case where β is a constant corresponds to Blum's grassfire [5], where the skeleton is the set of "quench" points of a fire front moving parallel to the shape's boundary (Fig. 4, top left). Technically, curves evolving under the constant- β case develop shocks, or entropy-satisfying singularities. Shocks provide a coloring of the

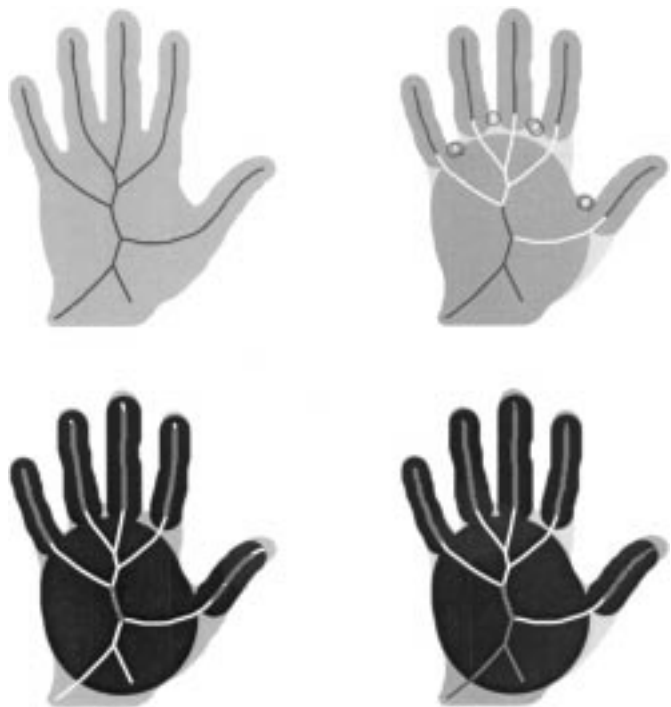


FIG. 4. (Top left) The original shape with skeleton (black lines). (Top right) The detected ligature (white lines), with reconstruction (dark grey region) of remaining skeleton (black lines), superimposed on the original shape (light grey region). The circles are ϵ -neighborhoods around the negative minima of curvature. (Bottom left) The detected seeds (high-order shocks) of shape (grey lines), reconstructed to the black region. (bottom right) The combination of seed (black region) and nonligature (dark grey region) reconstruction.

skeleton, according to the local variation of the radius function.⁶ To illustrate the coloring, imagine traversing a path along the skeleton. At a 1-shock the radius function varies monotonically, as is the case for a *protrusion*. At a 2-shock the radius function achieves a strict local minimum such that the medial axis is disconnected when the shock is removed, e.g., at a *neck*. At a 3-shock the radius function is constant along an interval, e.g., for a *bend* with parallel sides. Finally, at a 4-shock the radius function achieves a strict local maximum, as is the case when the evolving curve annihilates into a single point or a *seed*.

These bends and seeds can be used to provide a coarse-level description of an object. Bends and seeds are computed as follows. Within a branch, skeletal points are labeled “bends/seeds” where the corresponding boundary tangents are approximately parallel (angular difference $\leq 10^\circ$), while endpoints and junctions are labeled “bends/seeds” when they are local maxima of the maximal disk radius. In Fig. 4 (bottom left), the reconstructed⁷ bends and seeds (black), as predicted, give a surprisingly useful coarse description of the hand.

Unfortunately, bends and seeds do not faithfully represent all of the significant regions of a shape. In particular, notice how the tips of the fingers and the heel of the hand are missing in the bend/seed reconstruction (Fig. 4, bottom left). And yet, since some skeleton regions seem unstable (Fig. 10 and Section 1), it is undesirable to depend on all of the remaining skeleton. To guide the selection of other relevant skeleton regions, we suggest that ligature be removed.

An analysis of the evolution of the skeleton under general boundary motions [3] provides a mathematical basis for a connection between the instability of the skeleton and ligature. In particular, we consider the motion of the boundary of an object evolving under the geometric heat equation, or curve-shortening flow [12], where $\beta(\kappa) = \kappa$ in Eq. (1). The corresponding skeleton axis also satisfies a related geometric heat equation and is thus well-behaved. For example, the number of inflection points along a skeleton branch is a nonincreasing function of evolutionary time. However, the analysis reveals the nature of two internal $t = 0$ instabilities of the skeleton. The first is related to semiligature (Fig. 5):

PROPOSITION 1. *Suppose q is a point of the skeleton at $t = 0$, with $\pi(q) = \{a, b\}$, and the curvature $\kappa(a)$ at boundary point a is finite. If the boundary C of a planar object evolves via the geometric heat equation $\frac{\partial C}{\partial t} = \kappa N$ and $\kappa(b) \rightarrow -\infty$ at $t = 0$, then $\|\frac{\partial q}{\partial t}\|_{t=0} \rightarrow \infty$.*

The second instability is related to full ligature.

⁶ Blum’s pioneering work [5, 6] included a rich set of proposals for categorizing various regions of the skeleton based on differential properties of the radius function and axis curve. Unfortunately, his classification was largely ignored and no comprehensive computational results were ever presented. Shocks represent a coarse, but reliable, subclassification.

⁷ The reconstruction from a given subset of the skeleton is the union of the maximal disks corresponding to the points of that subset.

PROPOSITION 2. *If the boundary C of a planar object evolves via the geometric heat equation $\frac{\partial C}{\partial t} = \kappa N$, then the distance between two nearby three-branch skeleton junctions can decrease.*

See Fig. 5; exact specifications which describe Proposition 2 can be found in [3]. When the distance between two three-branch junctions decreases to zero under boundary smoothing, the topology of the skeleton may “switch” in the same way that the skeleton topologies on the left and right of Fig. 10 differ. When boundary perturbations are modelled with curve evolution, these results provide a theoretical basis for the empirical observations of ligature instability demonstrated in this paper. Note that the hierarchy induced by the branching structure in ligature regions is highly sensitive to the precise placement of negative curvature regions along the shape’s boundary (e.g., the light grey region between the fingers in Fig. 4). Returning to Marr’s principle [21], slight perturbations of the shape’s boundary at these negative curvature regions will have drastic effects on the topology of the skeleton.

Thus we seek to identify ligature regions in order to avoid these instabilities. The algorithm we used to compute ligature for a shape represented by a binary image is:

1. Compute skeleton S .
2. Compute $\pi(q)$, $\forall q \in S$.
3. Compute V as the set of negative minima of the signed curvature function along the boundary.
4. $\forall p \in \partial A$, label p as a concave corner iff there is a negative curvature minimum within an ϵ -ball⁸ around p .
5. $\forall q \in S$, label q as full ligature iff $\pi(q) \subset V$ or as semiligature iff $a \in V$, $b \notin V$, when $\pi(q) = \{a, b\}$.

We shall not pursue here the distinction between full and semiligature, for both are embroiled in the internal instability of the skeleton. The term *ligature* shall refer to the union of both full and semiligatures.

The computation of the skeleton can be based either on Voronoi or on curve evolution techniques (the examples here use code⁹ by Ogniewicz [24]). For both methods, the computation of the projection is essentially free. Implementations based on discrete thinning algorithms are more complex, requiring the propagation of boundary labels along the boundary to compute the projection. The negative minima of curvature were computed by measuring tangent changes along a piecewise circular approximation of the boundary.¹³

To see our ligature computation¹⁰ in action, consider Fig. 4. First observe the complicated junction structure of the skeleton

⁸ $\epsilon = 5$ pixels for all of the examples.

⁹ All examples were computed using the smoothed chord residual, with $\sigma = 1.0$.

¹⁰ The computational complexity of the above algorithm is $O(\max(p, n))$, where p is the number of boundary points and n is the number of skeleton points, given the precomputed skeleton and the negative curvature minima. The skeleton and curvature extrema computations have complexity $O(p \log p)$ and $O(p)$, respectively.

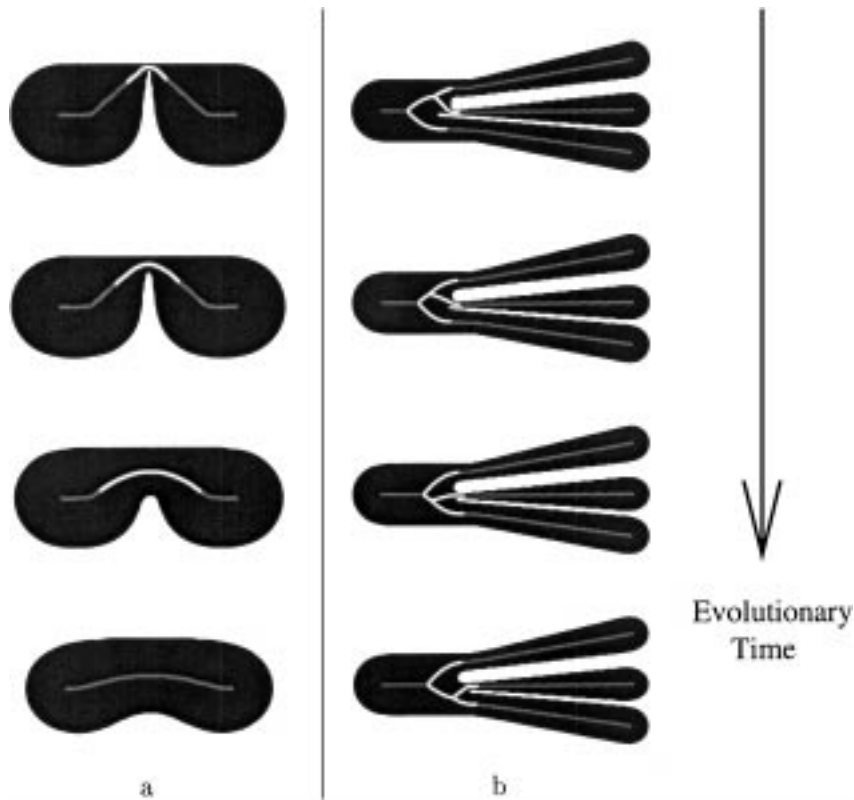


FIG. 5. Unstable examples of the evolution of the skeleton under boundary smoothing via the geometric heat equation. (a) Singular skeleton motion at semiligature: the concave corner causes extremely high skeleton normal velocity, as seen in the rapid flattening of the skeleton in this semiligature region. (b) Unstable 4-branch junctions: initially, the top and middle fingers join at the upper 3-branch junction. Under boundary smoothing, this junction momentarily passes through the left 3-branch junction to join the middle and bottom fingers.

within the palm. The detected ligature, which contains the sensitive internal skeletal structure, derives simply from the fact that maximal disks along it touch at least one of the detected concave corners. The reconstruction of the nonligature skeleton (top right) covers most of the shape, providing information that *protrudes into* even the tips of the fingers and heel of the hand (see Section 5). When combined with bends and seeds (Fig. 4), we see a full representation of the shape, including both coarse (palm, fingers) and detailed (wrist, finger tips) information.

4. RESULTS

In Figs. 6 and 7, we have a number of examples of the reconstruction of shapes from nonligature. These reconstructions show how nonligature includes a great deal of shape information, without the sensitive internal structure. In the top left two objects of Fig. 7, observe that a “shearing” of the plus sign pathologically causes a bifurcation of a four-branch junction into two three-branch junctions. Once ligature is identified, this instability in the junction is eliminated. A similar phenomenon occurs for a walking lizard.

Also evident in Figs. 6 and 7, however, is the incompleteness of the nonligature reconstruction. For example, notice how the nonligature does not reconstruct the legs of the panther or

walking lizard very well, due to the finite size of the ϵ -ball around negative curvature minima. In Figs. 8 and 9, we show a reconstruction of the *union* of nonligature and bends/seeds. It is critical to include this shock-based information for a complete view of the shape. For example, in the tail of the panther (see Fig. 6), where ligature is detected due to high curvature, it is the detected bend which compensates (Fig. 8) by overlapping the ligature region. Conversely, the seed in the leaf on the branch (Fig. 6) requires the nonligature skeleton for a richer description than a simple disk. Thus this combination of representations is more reliably detected than either one alone.

The example of the elephant (Fig. 8) emphasizes another aspect of our representation: *the resultant branches have a scale commensurate with each part*. Observe that while the (long) trunk corresponds to a long branch, the lip corresponds to a mere blip in the remaining skeleton. The misleadingly long ligature leading to the lip has been correctly removed.

This idea of ensuring that branches scale intuitively with the size of a part was exhibited in alternative axial representations of shape, such as smooth local symmetries (SLS) [7, 26] or the midpoint locus [11]. Since SLS is defined as the set of midpoints between pairs of mirror symmetric boundary tangent elements, it has the stable property that each SLS axis is never longer than the corresponding portions of boundary, unlike the skeleton, for

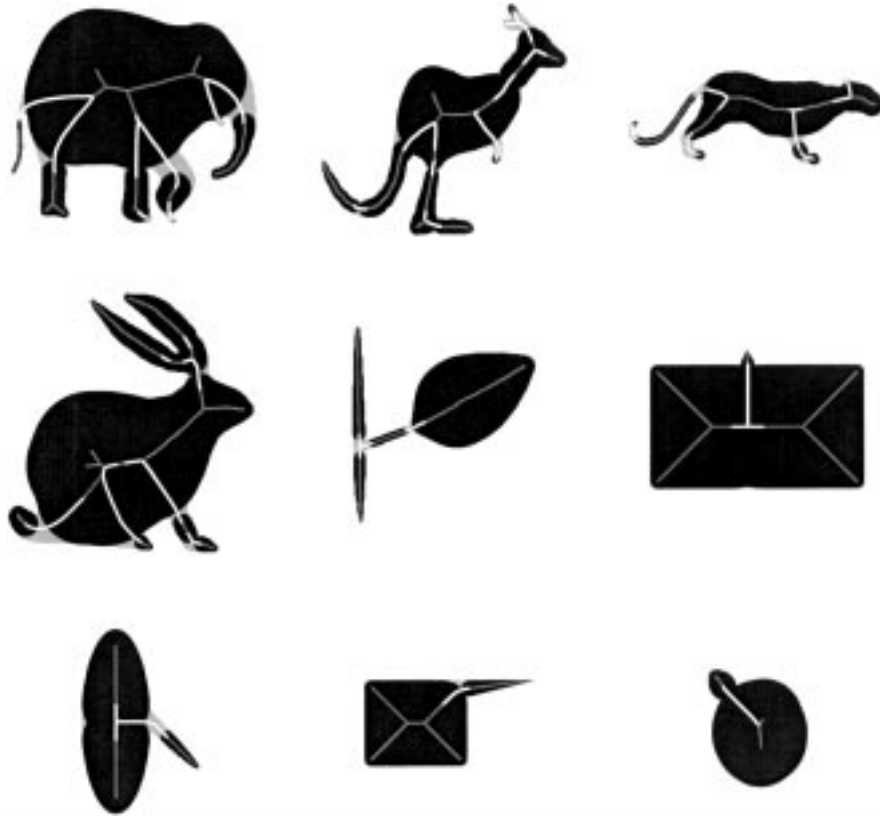


FIG. 6. A variety of shapes with ligature regions (white lines only) of the skeleton (grey and white lines) identified. Nonligature reconstructs to black region; the remaining region is shown in grey.

which the ratio (BAR [6]) of boundary length (B) to axis length (A) may become zero, e.g., the linkages from the finger bases to the palm in Fig. 12. While “velocity-based” pruning strategies [10, pp. 359–361] may remove some of these regions, ligature

does so specifically since it corresponds to $\text{BAR} = 0$. Philosophically, the use of SLS is not motivated by a perceptual organization principle beyond symmetry, whereas ligature is understood as directed growth (Section 5). In addition, proponents of SLS have combined them with other symmetries, either rotational [8] or parallel [33, 26], although it is unclear whether this can be done in a principled fashion. More importantly, the branches of the SLS, as well as generalized cylinders [23, 9], are not connected together to form a graph, unlike the skeleton (Fig. 12). Constructing joins among SLS axes is “the least mathematically well-founded part of SLS theory” [8, p. 111], and yet doing so could allow the computation of hierarchies to support generic object recognition. Such connectivity is free with the skeleton.

Returning to an example described in Section 1, we performed an experiment with a variety of hand images. Human subjects (students in the Center for Computational Vision and Control at Yale) aligned their hands on a white piece of paper and images were obtained using a Sony CCD camera. These grey-scale images were then thresholded to obtain the objects to be analyzed (Fig. 10, top). Observe how in the left column of the box in Fig. 10, the skeleton branches from the fingers merge differently than in the right two columns. Whereas this topological variability can affect abstraction hierarchies derived from the skeleton, the removal of ligature regions mitigates its effects. To illustrate, Fig. 11 (middle row) depicts the shock graphs [30] for the leftmost two hand shapes in the top row of Fig. 10. The

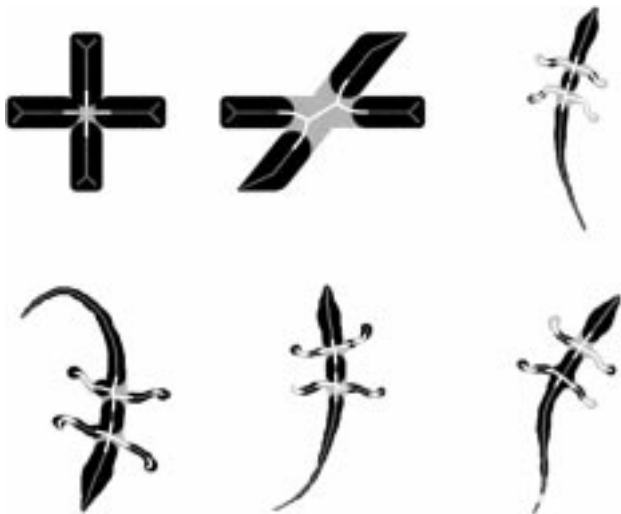


FIG. 7. (Top left) An internal skeleton branch is created when an object with a four-branch junction is “sheared” (cf. [34]). Ligature eliminates this topological change. (Top right and bottom) The skeleton of a lizard also undergoes topological changes as it walks (note junction alterations).

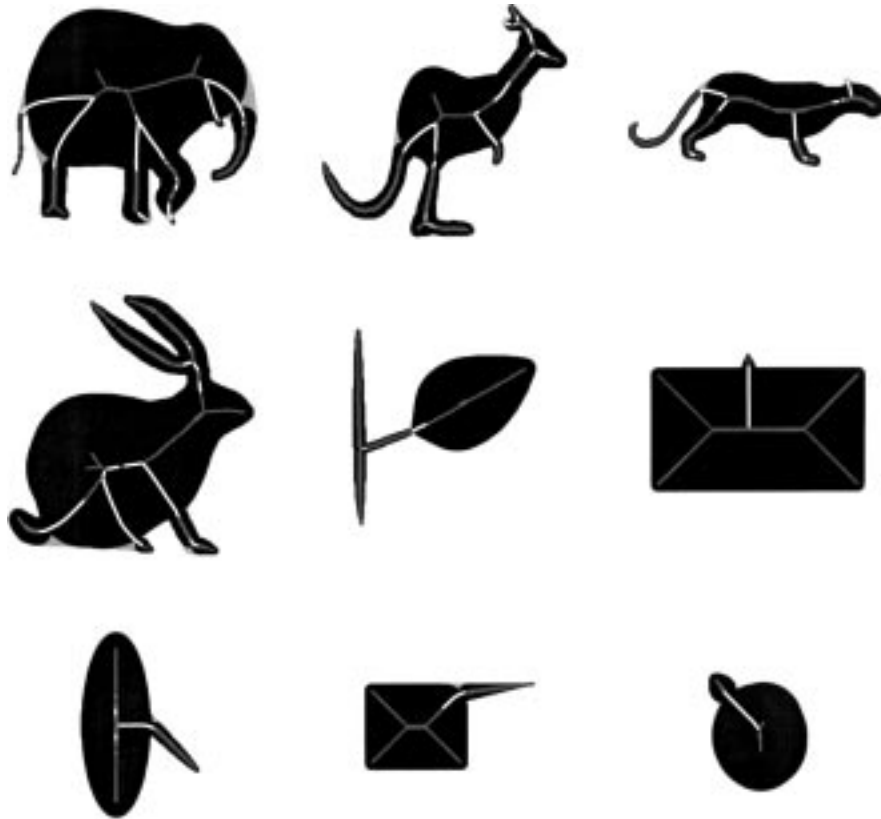


FIG. 8. A complete shape description is obtained when bends and seeds are combined with nonligature. Observe in the top row how shape regions that were eliminated by ligature (cf. Fig. 6), such as the legs in the elephant, kangaroo, and panther are compensated for by bends/seeds while still revealing the part structure described in Section 5.

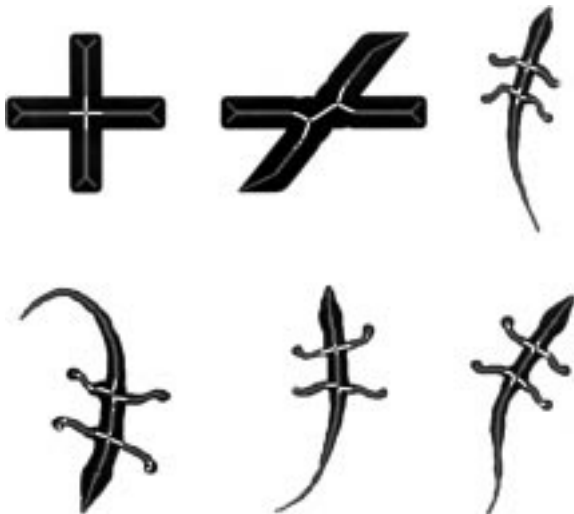


FIG. 9. Further examples of how a complete shape description is obtained when bends and seeds are combined with nonligature (cf. Fig. 7). (Top right and bottom) Observe considerable improvement in legs: bends now reconstruct most of the area that was lost in Fig. 7 due to the ϵ -ball used for detecting ligature.

nodes corresponding to the fingers are numbered from 001 to 005, in a clockwise direction starting from the little finger. When an ordering of the edges from each node is assigned, these shock graphs differ.¹¹ Shaded nodes correspond to ligature regions that are not bends or seeds. Observe that after these are removed, the two graphs become identical (bottom row), facilitating the process of object matching.

Finally, observe that the region *not* represented by the union of the bend/seed and nonligature skeleton reconstructions (grey regions in Figs. 8 and 10) is merely a way of visualizing the linkage between parts, a kind of perceptual glue of shape. We claim that only the functional linkage (e.g., via pointers) suggested by the perceptual glue need be represented, and further, that the actual skeletal branches representing this glue are the most sensitive internal regions of the skeleton.

5. INTERPRETATION: PARTS FROM GROWTH

Boundary glitches were considered as “noise” in Section 1, but syntactically similar configurations could also denote parts such as limbs or tails [29, 31]. This suggests a closer look at how

¹¹ However, these graphs are topologically identical.



FIG. 10. (Top) Grey-scale image obtained for topological sensitivity experiment (see text). (Bottom box) Similar shapes with distinct internal skeleton topologies (compare left to right two columns). Grey lines represent combined bends/seeds and nonligature. Note how ligature (white) highlights the topologically distinct skeleton regions, making explicit (in the remaining skeleton) the perceptual similarity of all these objects.

limbs might arise. In particular, let us consider how objects grow. In Fig. 13, the early development of the amphibious plant *Prosperpinaca palustris* clearly shows an outward branching from an initial “body.” Notice how negative curvature zones are present at the bases of the branches. At the earliest stages of growth (Fig. 13), an internal “growth seed” in a young willow suddenly develops as a branch root, pushing through the body and creating two negative curvature zones. This *source* of growth makes the joining of the root to the body explicit, leading to an explanation of parts via a *shared growth region*, where part decomposition is viewed as a kind of inverse to physical growth:

PRINCIPLE OF PERCEPTUAL GROWTH. FORWARD: *Suppose an object undergoing rapid and directed outward growth is given.*

The result is a silhouette whose boundary has negative curvature zones.

INVERSE: *Suppose the silhouette of a mature object is given. Part decomposition entails the association of negative curvature zones with an internal region which could have been the source of an outward growth.*

The connection between negative minima of curvature of the boundary and the perception of parts was first noted by Hoffman and Richards [14]. Related work which incorporates properties of the shape’s interior includes part definitions in terms of skeleton junctions [6], second-order shocks [17], degenerate waves¹² [32], part-lines [29], and part-cuts [15]. The latter two proposals advocate a strict partitioning of a shape into disjoint regions and suggest a number of criteria by which the salience of the constituent parts may be evaluated. Here we depart from the view that parts should be *disjoint* sets, as the principle of perceptual growth leads to an equivalent account of the decomposition of interpenetrating objects in terms of a “shared region” or *virtual join*. For instance, consider the silhouette of an arrow in your chest: the region in your body taken up by the arrow is exactly the region in your body that is the source of your suffering (“sharing” is not always equal). Fig. 2 (top) shows such an interpenetration. Zhu and Yuille have also made use of a similar idea of overlap at joints of bones [34]; however, like Blum and Nagel, they view each skeleton branch as a distinct part, even though convex objects—clearly perceptual units—may have many branches.

In an attempt to provide a causal explanation of a part as the outcome of a “protrusion” process acting on a shape’s boundary, Leyton too has argued against segmentation approaches to partitioning: “. . . a part is not a rigid segment: A part is a *process*! It is a *temporal* or causal concept” [19, p. 363]. We note that this protrusion-to-parts transition is signalled by the appearance of a ligature region in the shape’s skeleton. In particular, since a salience criterion,¹³ such as a threshold on curvature [14], must be introduced to locate negative curvature minima, “unsalient” minima will not be detected, and in this circumstance ligature will not form. The consequence of this detection process is the semantic distinction between a protrusion (Fig. 14 right) and a part (Fig. 14 left). A similar phenomenon is observed for a sequence of a rotating coffee cup as the handle comes into view [29, p. 243].

In addition to the *anisotropic* growth described above, one can consider a more primitive *isotropic* form of growth. Isotropic growth could emerge simultaneously along a curve (as a bend), or at discrete points (as seeds). Technically, such a growth front is a union of circles via Huygen’s principle, and arises in the

¹² Degenerate waves are a rephrasing of Blum’s ligature concept using curve evolution terminology.

¹³ In our current implementation, negative minima of curvature where the absolute value of the curvature is above a threshold will be detected. Other schemes that define part salience using a notion of the “mass” or “extent” of a part [29, 31] could also be invoked.

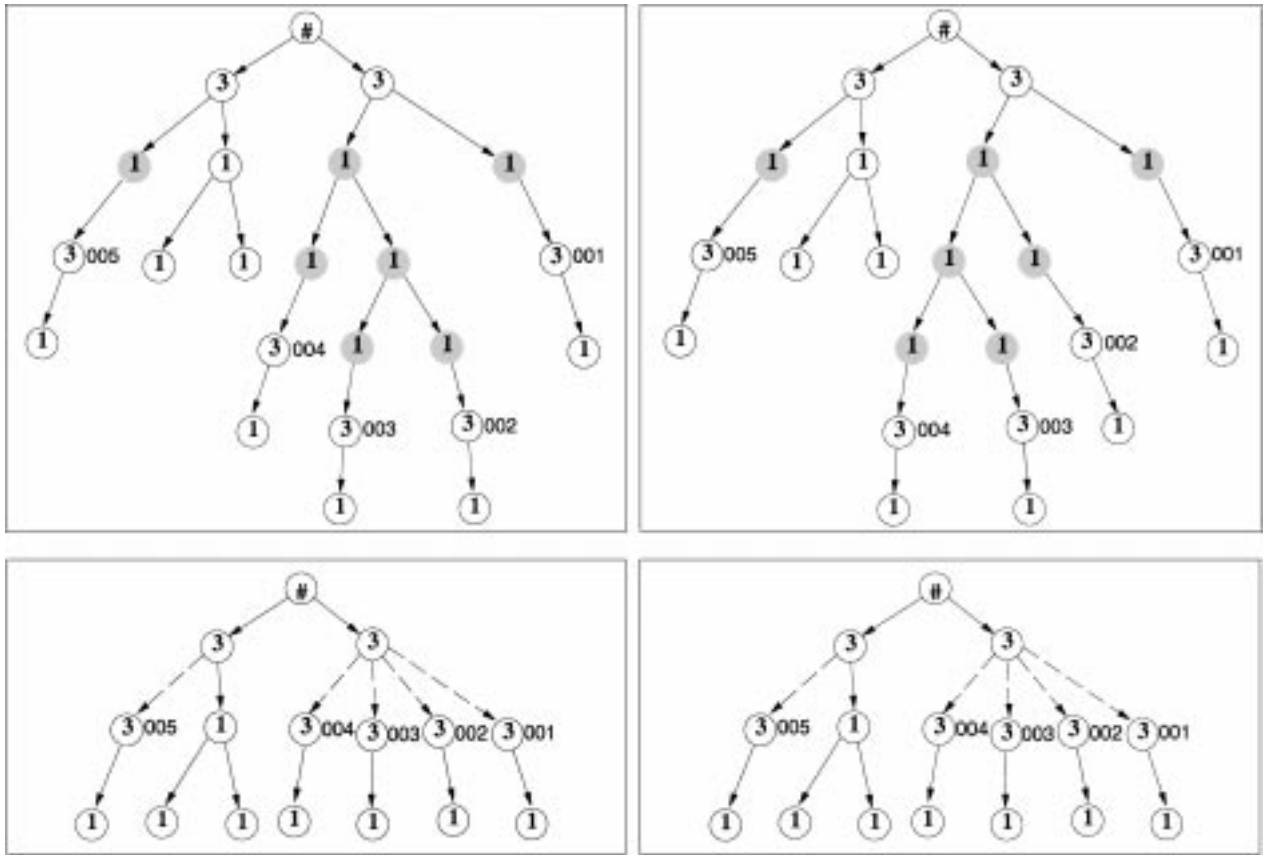


FIG. 11. Distinct shock graphs (top) resulting from distinct skeleton topologies of leftmost two hands of top row of Fig. 10. Shaded nodes correspond to ligature regions which are not bends or seeds. After these are removed, the shock graphs become identical (bottom); the dashed lines represent structural links.

theory of curve evolution [17] as 3- and 4-shocks, respectively (see Section 3). Kovacs and Julesz have confirmed the perceptual significance of bends and seeds as anchor points in tasks involving shape perception [18]. In what follows we develop a connection between ligature regions and limb-, neck-, and tail-based parts as proposed in [29, 31].

5.1. *Limbs and Tails from Full and Semiligature*

To see how the notion of ligature leads to a skeleton-based limb, consider Fig. 15. First observe how both semiligature and full ligature make up a sizeable part of the skeleton of this shape: ligature makes explicit how the concave corners exert a

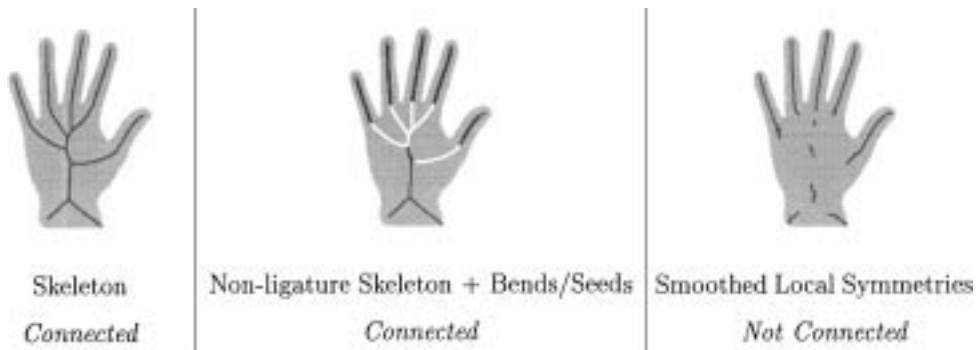


FIG. 12. Stability with connectivity in axial descriptions of shape. (Left) The Blum skeleton. Observe that the branches in the palm are much longer than the corresponding boundary. (Center) Our representation eliminates sensitive portions of the skeleton while maintaining connectivity, thus supporting a modular organization of shape. (Right) The subset of smoothed local symmetries (SLS) from the bitangent circles inside an object. Although the axes have length commensurate with the size of the corresponding shape structure, they are not joined together [8]. This problem is more acute when the full SLS is used.

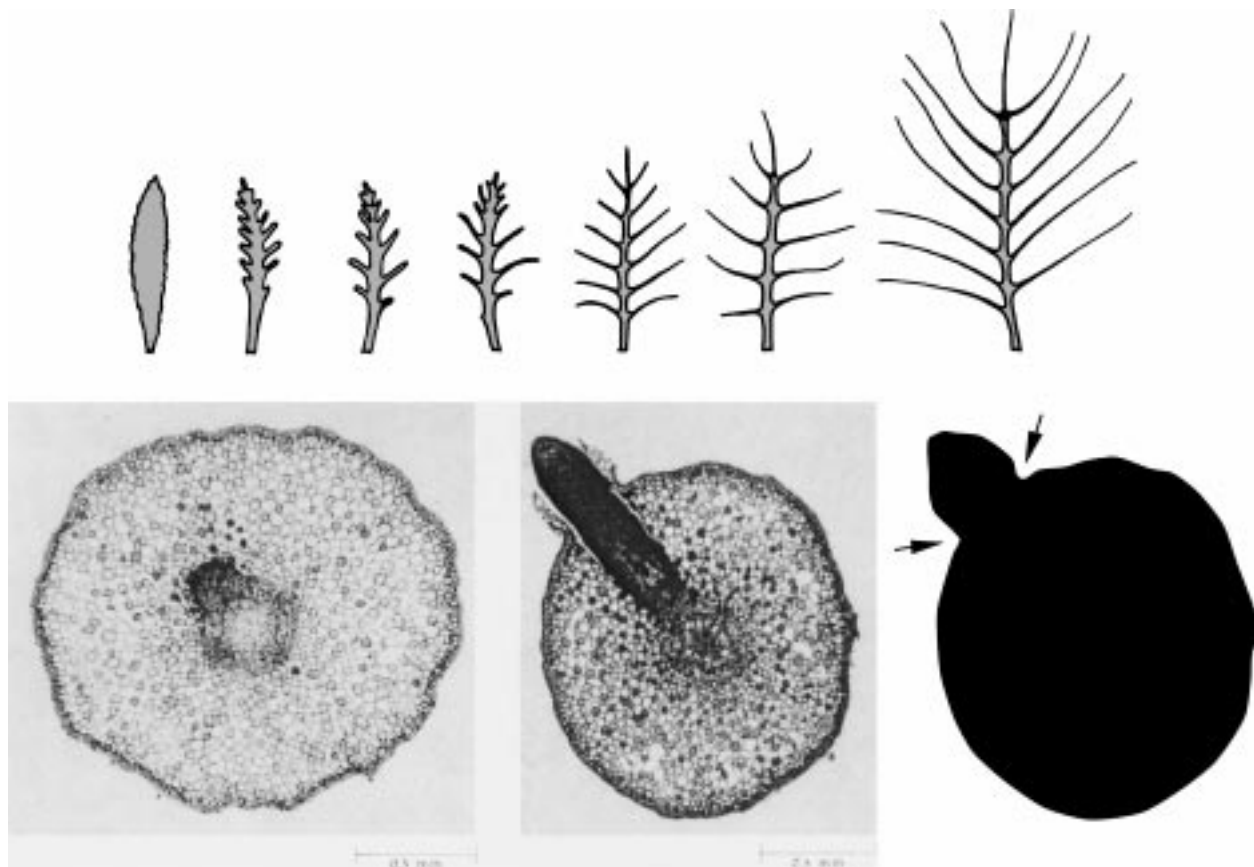


FIG. 13. (Top) The development of leaf forms (from left to right). Note that outward branching is accompanied by concave corners. (Bottom) The development of a branch root in a willow. (Left) Within the core, observe the source of the root as a specialized dark region. (Center) The root rapidly grows towards the top left, displacing the epidermis. (Right) The resulting silhouette with sharp negative curvature zones indicated with arrows.

significant influence over a shape *through its interior*. The full ligature $FL(a, b)$ with respect to concave corners a and b is a horizontal line segment that represents the linking of the ellipse on the left to the stick on the right. Otherwise full ligature has



FIG. 14. The nondetection of a negative curvature minimum as a part-to-protrusion transition. The ligature linking a part (the thumb) to the palm (left) disappears (right) when the negative curvature minimum is undetected as the part becomes a slight protrusion. Observe that the topologies of these two skeletons are identical, and so skeleton part-decomposition schemes based on junctions [6, 34] would not distinguish them. Coloring the skeleton by ligature, however, makes the part/protrusion distinction explicit.

no role in describing the shape; indeed, full ligature is constituted by skeletal points related to only a single pair of boundary points.

Thus full ligature divides the skeleton into two separated parts, leading to skeletal descriptions of the parts themselves, after the full ligature itself is discarded. Now we can separately regenerate the parts that those *subskeletons* represent using maximal disks whose radii are stored in the radius function. For the ellipse we observe that all of the boundary of the ellipse is recovered, except an arc between a and b which arises as a kind of “upper bound” on the true shape (Fig. 18, right). The recovered stick also has all of the contour of some “undamaged” stick except for that lost inside the ellipse, which is regenerated as a kind of knobby end. When we put these two regenerated forms back together we get the *virtual join* as their intersection; this virtual join can be viewed as a physically shared region where growth began, corresponding to the principle of perceptual growth. Note how the bulk of the virtual join is due to displacement by the stick which grew out from the ellipse. Finally, since the radius function is increasing along the full ligature *from* the stick *to* the ellipse, the stick is thus slave, child, or indeed limb to the larger ellipse as master, parent, or body, expressing the idea of a hierarchy of shape [17]. If the radius function has a local minimum

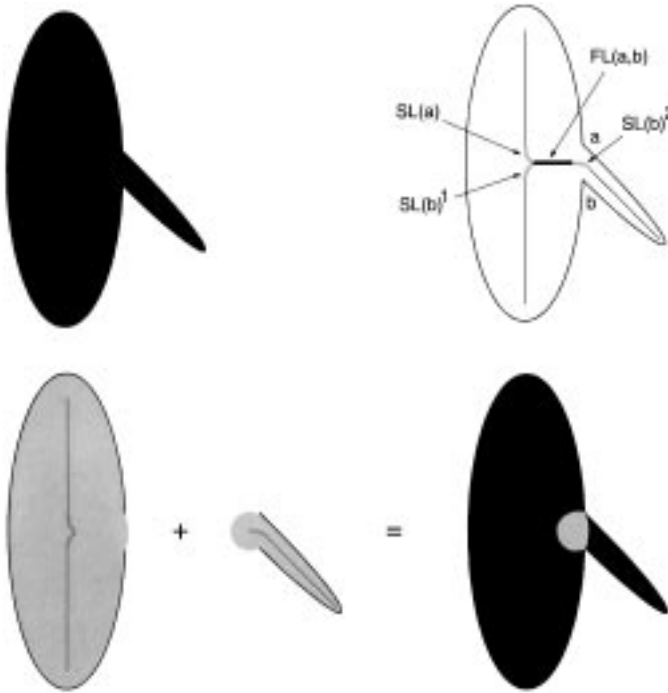


FIG. 15. Limb from full ligature. An ellipse with a protruding limb (top left) is shown with its skeleton (top right). Full ligature is in bold, semiligature is in grey, and the remainder of the skeleton is depicted with thin lines. Superscripts are used to distinguish several connected components of semiligature with respect to the same endpoint. (Bottom) The shape is expanded into its constituent parts. (Bottom left) Here the two semiligature branches on the left, $SL(a)$ and $SL(b)^1$, remain with the ellipse to give an “upper bound” to the original ellipse, while the semiligature branch $SL(b)^2$ on the right is associated with the stick (bottom center). Thus in the formation of a whole object, information about its constituent parts is lost, leading to the virtual join region (shown in grey, bottom right). This is another definition of the limbs described in [29, 31].

(second-order shock), then the parent–child relationship is lost and we are left with an “equal” decomposition at a neck.

Unfortunately the notion of a limb is too restrictive. For example, the tail of a kangaroo is perceptually triggered by a sin-

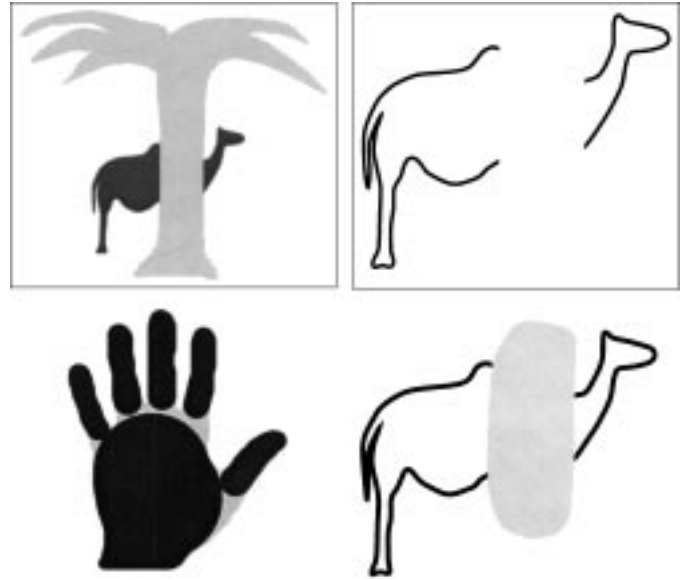


FIG. 17. (Top left) The bounding contour of a camel is broken by a foreground palm tree. (Top right) Curve fragments of the occluded object. (Bottom row) The duality between part decomposition and fragment grouping: two kinds of “glue.” Whereas in part decomposition we must remove “glue” (left, in grey) to expose the part structure, in grouping we must add “glue” (right, in grey) to bind the fragments together. Notice that the perceptual glue here (left) differs from the virtual joins in Figs. 15 and 16. The virtual join of the hand would extend well into the palm, corresponding to the joints connecting the fingers to the palm.

gle concave corner [31]. This phenomenon requires a formal description. To construct an appropriate skeleton-based definition of a tail, one might consider letting a tail be induced by a branch of semiligature, as it relates skeletal points to a single concave corner. Unfortunately tails are more subtle, for full ligature branches will typically arise with abutting semiligature components with respect to the same concave corners (Fig. 15). Nonetheless, the use of semiligature for defining a tail is promising (see Fig. 16).

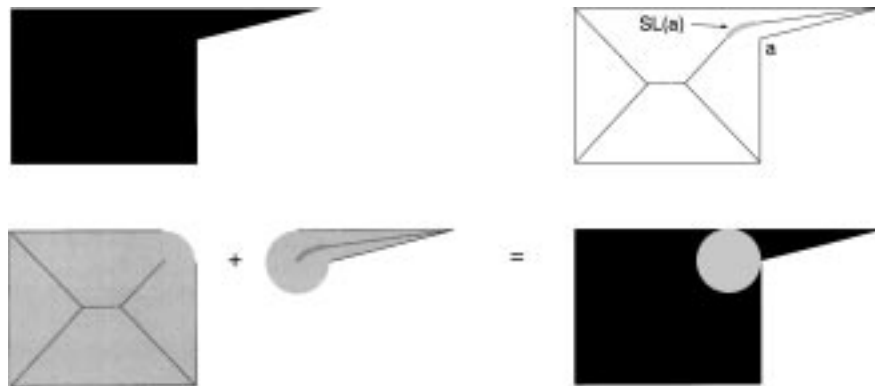


FIG. 16. A tail from semiligature. An object (top left) and its skeleton (thin lines) with semiligature (grey) with respect to corner a (top right) is shown. The lone semiligature triggers the breaking of the skeleton into parts (bottom left), where the corresponding regions are generated using maximal disks. (bottom right) The join region (grey) is defined as the intersection of the regenerated regions. This construction was inspired by [29, 31].

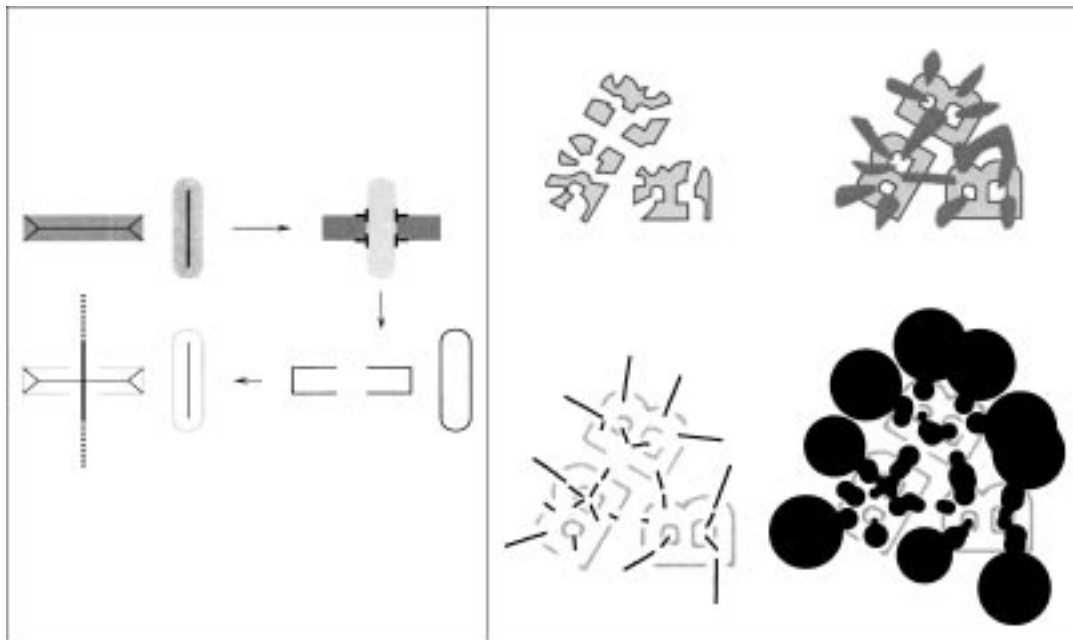


FIG. 18. (Left box) Grouping using the gap skeleton [2]. Objects with skeletons (top left) are brought into an occlusion relationship (top right). (Bottom right) Rectangle fragments are “farther” than occluder boundary, due to T-junctions, but whether they arise from the same object is unknown and defines the contour fragment grouping problem. (Bottom left) Note the similarity between the gap skeleton (thick vertical line) and skeleton of the occluder; consider the gap skeleton as representing a “virtual occluder”. (Right box) Fragment grouping is related to the perception of occluders. Apparently unrelated pieces (top left) are seen as three B’s when occluders are present (top right). (Bottom left) Contour fragments of occluded B’s (grey) are linked using gap skeleton (black lines), which when reconstructed give virtual occluders (black region) which approximate a covering of actual occluders and unconstrained space.

Here we have considered the question of what kind of information from the skeleton, beyond being a mere set of points, might be useful. Shocks have provided a basis for defining significance in a hierarchical shape description, while ligature has provided a basis for shape decomposition. Both kinds of skeleton “coloring,” and perhaps others, play a role in understanding shape.

6. DUALITY BETWEEN PART DECOMPOSITION AND FRAGMENT GROUPING

Occlusion is a genuine cause of edge fragmentation (Fig. 17, top), and one goal of grouping is to collect these contour fragments into groups, each one of which is to be associated with a single object. Here we consider how a new understanding of grouping arises in a manner dual to the part decomposition described earlier. There, after a process of *removing* the binding region (“perceptual glue”), what remains are the parts of an object. For the grouping of contour fragments, we shall *add* a kind of perceptual glue, called a virtual occluder, as a trigger for linking the fragment endpoints together. Observe how these regional operations are complementary (Fig. 17, bottom).

Our approach [2]¹⁴ to fragment grouping begins with the observation that occluders create contour gaps so large that good continuation is inappropriate. Rather, we view long-distance fragment grouping as kind of inverse to physical occlusion:

PRINCIPLE OF PERCEPTUAL OCCLUSION. FORWARD: *Given a collection of objects distributed in space, occlusion will arise generically under projection onto images. The result is a composite bounding contour which, by transversality [14, 16], will contain discontinuities at T-junctions. Consequently, the bounding contours of occluded objects may be fragmented in the image.*
INVERSE: *Suppose a collection of contour fragments is given. Long-distance contour fragment grouping is the association of fragments that could have been the result of the occlusion of a single object by some occluder.*

However, since many occluders might equally account for an observed fragmentation, this inverse problem is ill posed [13], and so we will prefer simple to complex shapes for the occluder. Thus a pair of fragment endpoints should be linked only if some simple occluder could have produced them. We formalize this *shared, simple occlusion* (SSO) constraint using gap skeleton, which may be defined as that full ligature with respect to a pair of endpoints¹⁵ which contains the midpoint between them (Fig. 18). Geometrically, we have a gap skeleton with respect to a given pair of endpoints if we can fit a disk centered between them, a disk which is a crude representation of a simple, blob-like occluder. Thus, by the principle of perceptual occlusion *the appearance of a gap skeleton between two endpoints is a necessary condition for their linking together.*

¹⁴ Deleted in proof.

¹⁵ Endpoints may be thought of as degenerate corners.

Observe how the principle of perceptual growth (Section 5) describes a weak form of occlusion: the negative curvature zones in the boundary of a silhouette are just smoothed versions of concave corners, and these concave corners are degenerate T-junctions, because the contrast between objects in an occlusion relation is lost. The objects which make up a composite whole as a silhouette are thus viewed as being at the same depth, unlike objects in occlusion. Thus the growth principle is dual to the principle of perceptual occlusion which explicitly invokes an implicit occluder among contour fragments to be grouped, much like the shared growth region in part decomposition. Thus whereas in shape decomposition we seek a virtual join to explain the *linking* of parts, in grouping we seek a virtual occluder to explain the *separation* of fragments.

7. CONCLUSION

In this paper we have described how the long-standing problem of the internal instability of the Blum skeleton might be alleviated by identifying ligature, a distinct region of the skeleton. The deletion of ligature regions leads to stable hierarchical representations for indexing object databases. We have interpreted ligature using a principle of perceptual growth which suggests that at least certain aspects of part decomposition require *both* explicit evidence (corners) and an implicit place (perceptual glue or virtual join). Finally, we have observed a duality between the problems of part decomposition based on directed growth and contour fragment grouping based on shared, simple occluders [2].

Blum's skeleton is interesting because it provides a language for defining a hierarchical representation of planar shapes. Shocks expand on skeletons in one way, by making explicit their classification and significance; ligature expands on skeletons in another, by addressing stability. It remains to be seen whether other properties of the skeleton can be exploited for generic object recognition.

ACKNOWLEDGMENTS

We thank Shamez Alibhai, Ohad Ben-Shahar, Athinodoros Georghiades, and Patrick Huggins for helpful discussions and the reviewers for inspiring us to include Figs. 12 and 14. We also gratefully acknowledge the support of AFSOR, NSERC, and FCAR for funding this research.

REFERENCES

1. J. August, *From Contour Fragment Grouping to Shape Decomposition*, Master's thesis, McGill University, August 1996.
2. J. August, K. Siddiqi, and S. W. Zucker, Contour fragment grouping and shared, simple occluders, *Comput. Vision Image Understanding* **76**(2), 1999.
3. J. August, A. Tannenbaum, and S. Zucker, On the evolution of the skeleton, in *Proc. Int. Conf. Computer Vision*, 1999, pp. 315–322.
4. I. Biederman, Recognition-by-components: A theory of human image understanding, *Psychol. Rev.* **94**, 1987, 115–147.
5. H. Blum, Biological shape and visual science, *J. Theor. Biol.* **38**, 1973, 205–287.
6. H. Blum and R. N. Nagel, Shape description using weighted symmetric axis features, *Patt. Recogn.* **10**, 1978, 167–180.
7. M. Brady and H. Asada, Smoothed local symmetries and their implementation, *Int. J. Robot. Res.* **3**(3), 1984, 36–61.
8. M. Brady and G. Scott, Parallel algorithms for shape representation, in *Parallel Architecture and Computer Vision* (I. Page, Ed.), pp. 97–118, Oxford Univ. Press, Oxford 1988.
9. R. Brooks, Symbolic reasoning among 3-d models and 2-d images, *Artif. Intell.* **17**, 1981, 285–348.
10. R. O. Duda and P. E. Hart, *Pattern Classification and Scene Analysis*, Wiley, New York, 1973.
11. P. J. Giblin and S. A. Brassett, Local symmetry of plane curves, *Amer. Math. Monthly* **92**, 1985, 689–707.
12. M. A. Grayson, Shortening embedded curves, *Ann. Math.* **129**, 1989, 71–111.
13. J. Hadamard, *Lectures on the Cauchy Problem in Linear Partial Differential Equations*, Yale Univ. Press, New Haven, CT, 1923.
14. D. D. Hoffman and W. A. Richards, Parts of recognition, *Cognition* **18**, 1985, 65–96.
15. D. D. Hoffman and M. Singh, Saliency of visual parts, *Cognition* **63**, 1997, 29–78.
16. P. J. Kellman and T. F. Shipley, A theory of visual interpolation in object perception, *Cognitive Psychol.* **23**, 1991, 141–221.
17. B. B. Kimia, A. R. Tannenbaum, and S. W. Zucker, Shapes, shocks, and deformations, I, *Int. J. Comput. Vision* **15**, 1995, 189–224.
18. I. Kovacs and B. Julesz, Perceptual sensitivity maps within globally defined visual shapes, *Nature* **370**, 1994, 644–646.
19. M. Leyton, Inferring causal history from shape, *Cognitive Sci.* **13**, 1989, 357–387.
20. T. Liu, D. Geiger, and R. Kohn, Representation and self-similarity of shapes, in *Proc. Int. Conf. Computer Vision*, 1998, pp. 1129–1135.
21. D. Marr, *Vision*, Freeman, New York, 1982.
22. H. Murase and S. Nayar, Visual learning and recognition of 3-D objects from appearance, *Int. J. Comput. Vision* **14**, 1995, 5–24.
23. R. Nevatia and T. O. Binford, Description and recognition of curved objects, *Artif. Intell.* **8**, 1977, 77–98.
24. R. L. Ogniewicz, *Discrete Voronoi Skeletons*, Hartung-Gorre, 1993.
25. S. M. Pizer, W. R. Oliver, and S. H. Bloomberg, Hierarchical shape description via the multiresolution symmetric axis transform, *IEEE Trans. Pattern Anal. Mach. Intell.* **9**, 1987, 505–511.
26. H. Rom and G. Medioni, Hierarchical decomposition and axial shape description, *IEEE Trans. Pattern Anal. Mach. Intell.* **15**(10), 1993, 973–981.
27. D. Shaked and A. M. Bruckstein, Pruning medial axes, *Comput. Vision Image Understanding* **69**, 1998, 156–169.
28. D. Sharvit, J. Chan, H. Tek, and B. B. Kimia, Symmetry-based indexing of image databases, in *IEEE Workshop on Content-Based Access of Image and Video Libraries*, 1998.
29. K. Siddiqi and B. B. Kimia, Parts of visual form: Computational aspects, *IEEE Trans. Pattern Anal. Mach. Intell.* **17**(3), 1994, 239–251.
30. K. Siddiqi, A. Shokoufandeh, S. J. Dickinson, and S. W. Zucker, Shock, graphs and shape matching, *Int. J. Comput. Vision* **35**, 1999, 13–32.
31. K. Siddiqi, K. J. Tresness, and B. B. Kimia, Parts of visual form: Psychophysical aspects, *Perception* **25**(4), 1996, 399–424.
32. H. Tek, P. A. Stoll, and B. B. Kimia, Shocks from images: Propagation of orientation elements, in *Proc. Comput. Vision Patt. Recogn.*, 1997, pp. 839–845.
33. F. Ulupinar and R. Nevatia, Shape from contour: Straight homogeneous generalized cylinders and constant cross section generalized cylinders, *IEEE Trans. Pattern Anal. Mach. Intell.* **17**(2), 1995, 120–135.
34. S. C. Zhu and A. L. Yuille, Forms: A flexible object recognition and modelling system, *Int. J. Comput. Vision* **20**(3), 1996, 187–212.